

# XRD & SEM studies of Fly-ash and Phosphogypsum based Geopolymer Bricks

Jandhyala Jagmohan Vijay\*<sup>1</sup>, Prof Hanchate Sudarsana Rao\*<sup>2</sup>, Prof. Vaishali. G. Ghorpade\*<sup>3</sup>

\*<sup>1</sup> Research Scholar, <sup>2</sup>&<sup>3</sup> Professors. Civil Engineering Department, JNTUA, Anantapur. Andhra Pradesh, India.

<sup>1</sup>vijayjj1@gmail.com, <sup>2</sup>hanchate123@yahoo.co.in, <sup>3</sup>ghorpade\_vaishali@yahoo.co.in

**Abstract** - Ever since the dawn of humans on this earth, there has been a constant endeavour to build better shelters for various needs. Early man used to stay in caves, forests, and other natural dwelling places; as time passed and the human population increased, the need for cheaper accommodation, which can be built faster and can last longer, has increased. Eventually, Cement was rediscovered and has ever since being used as a versatile construction material. But the excessive use of Cement has impacted the environment and is known to have caused detrimental effects. Using eco-friendly alternatives in place of Cement is the need of the hour. It would be better if such eco-friendly materials used for construction were not mined, but if they were waste materials produced from other industrial processes. These industrial processes are unavoidable and shall continue to use for the betterment of humankind. These industrial processes have a lot of waste material that affect the environment causing air, water and soil pollution. These waste materials end up being discharged into water bodies, into the air, or ending up in landfills; they can produce eco-friendly alternative construction material like bricks and other cementitious material, eventually replacing the present material, which has a high level of waste environmentally detrimental effect. For the sake of this study, two such waste materials are identified. These materials are fly-ash and Phosphogypsum. When combined with alkaline substances like sodium hydroxide and sodium silicate, these materials produce a mixture with cementitious properties. This paste can be used to make construction materials like bricks, filler materials, and eventually, can be used as a replacement for Cement.

**Keywords:** Environment, Geopolymers, Phosphogypsum, Fly-ash, Diffraction.

## I. INTRODUCTION

Demand for better infrastructure due to the increased human population has increased construction activity. Since Cement has been used extensively throughout history for construction activity, its demand has risen to meet the infrastructure development. But extensive use of Cement has known to cause increased emission of CO<sub>2</sub> and other greenhouse gasses. Low carbon footprint building materials are the need of the hour, and geo-polymers may present us with an excellent alternative. Geo-polymers are non-organic synthesised polymer products consisting mainly of aluminium or silicate compounds; these may be naturally formed or synthetically formed in combination with fly-ash and other pozzolanic material. Structural properties like high tensile strength and compressive

strength, resistance to acid attack and sulphate, low water absorption, fire resistance etc., are some of the commonly exhibited properties of Geo-polymers.

It is essential to study microstructure properties in addition to macro-properties of these materials. An attempt has been made to corroborate the earlier studied macro-properties of masonry brick (made with Phosphogypsum) using microstructure analysis. For this study, the tools used are Scanning electron microscope (SEM) and X-ray Diffraction (XRD/EDX/PXRD).

## II. EXAMINATION OF CURRENTLY AVAILABLE LITERATURE

**Yootaek Kim and Kyongwoo Lee [1]** tested geopolymers with six different Si/Al ratios using a transmission electron microscope and concluded that they were exhibiting micro-crystallite structures with 80-100 nano-sized also nano crystallite structures of size 10-30 nanometres. The geo-polymerisation process may have caused these particles to form. High compressive strength may be a result of these crystals and crystallites. **Ahmad Muhd Izzat et al. [2]** studied geopolymer mortars and OPC (Ordinary Portland Cement) and concluded that both samples were prone to acid attack. The theory complies with weight shifts and power degradation. However, with a low percentage of weight changes and a decrease in strength of 3.66 and 24.13 per cent, geopolymer mortar was less vulnerable to acidic attack. OPC mortar showed abysmal performance; 18.5 and 69.26 per cent respectively in both weight changes and strength degradation. In the microstructural photos, the stability of both materials was detailed; The corroded part of the OPC mortar was revealed on the exposed surface. Stereo microscopic images showed significant degradation of OPC mortar, and SEM images showed the weakness of OPC mortar in acid solution due to the high calcium percentage of OPC. On the other hand, due to the absence of surface deteriorating symptoms in the geopolymer matrix, the micrographs analysis conformed the aluminosilicate network in geopolymer was less susceptible in acidic solution medium. **Abideng Hawa, Danupon Tonnayopas, Woraphot Prachasaree [3]**, Studied the effect of partially replacing Metakaolin with Oil Palm ash. They investigated the variance of microstructure and compressive strength of geo-polymer concrete subjected to heat curing for varying periods. Compressive strength has increased due to the mix having very little unreacted material and a compacted dense matrix. Higher compressive strength may also have been due to the formation of geo-polymers in the hot mixture and Si-Al reaction, which produced



aluminosilicate. **Oliver Vogt et al. [4]**, from the results of their studies, concluded that when 10 % fly-ash substitutes metakaolin, it improves workability and delays the time of settings, both initial and final, not much affecting the microstructure and strength properties of the geopolymer's, particularly at larger l/s(liquid/solid) ratio. Pore size distributions (porosimetry of intrusion by mercury) are comparable between metakaolin geopolymer (containing zero percentage fly-ash) and geopolymer (containing ten percentage fly-ash) only at an l/s ratio of 0.6. Lower l/s ratios majorly differentiate formulations between the two types of geopolymers. When fly-ash content is above 20 per cent, the variation in strength and porosity is more pronounced; pore size distribution variation is also widely seen at this percentage of fly-ash. Greater l/s ratio and greater fly-ash concentrations in geo-polymers are produced due to lower concentrations of Al, due to which heat evolved in the first 24 hours of reaction. **Mandeep Kaur, Jaspal Singh, Manpreet Kaur [5]** studied geopolymer mortar containing fly ash. When Nano metakaolin (NMK) proportion by weight of fly-ash was varied as 0, 2, 4, 6, 8 and 10, it was observed that the capacity of geopolymer mix moves toward higher side when cured for longer periods. 70-80 % of total compressive strength gained in 28 days of normal curing was noted after 72 hours of curing a nano-metakaolin integrated geopolymer mix in an ambient atmosphere. Up to 4 % replacement Nano metakaolin, the compressive capacity is high. After 4 % replacement, the rise in compressive capacity is very much low. The recovery period of 28 days produced a compressive capacity of 52.77 Mpa. It is evident from the SEM study that the increase in compressive capacity of the geopolymer (G.C.) mix containing fly-ash at 4% of Nano-metakaolin is due to the presence of aluminium oxide of NMK and silica. SEM research also brought to light that the geopolymer mix (GN-0) used for control has a lower density than the G.C. mix containing 4% NMK; this effect shall be attributed to the larger number of fly ash particles unreacted and partially reacted. Therefore, compared to geopolymer mixes with 4 per cent NMK, this contributes to lower compressive strength. EDS study reveals that with the introduction of NMK, the compressive capacity of the mix increases and the Si/Al ratio decreases. The lowered strength of the geopolymer mix results from a higher Si/Al ratio. The determination coefficient value ( $R^2$ ) is near one for the various healing ages of 3, 7, 14 and 28 days; this suggests the regression curve has a goodness of fit. **Diegles Simoes de Toledo Pereira et al. [6]** conducted a comparative study between the characteristics of mechanical, thermal behaviour and microstructure, of concrete made of geo-polymer (G.C.) and Cement of high performance (HPC-high Performance Portland cement)), which lead to a new finding, which could have wide applications in civil engineering. G.C. concrete just after 2 hours of age develops a good compressive strength. But HPC based geopolymer remains a paste and does not harden. Both concretes have similar compressive capacities when ageing time is from 7 days to 2 years; this leads to their application not only in building construction,

it also can be used for heavy loads like traffic pavements. Fractography shows aggregate with small pores and microcracks attached to a consistent single-phase geopolymer web. The 3-phase HPC matrix, on the other hand, reveals greater pores and fractures connected in conjunction with the aggregate web. XRD (X-ray Diffraction) analysis results support the predicted conversion of kaolinite crystal into amorphous metakaolin form, a key component of the Geopolymer concrete (G.C.) web. Microfractograph gives the interconnected porosity and microcracks, which is support by the above XRD study results. When DSC (Differential scanning calorimetry) and TGA (Thermogravimetric analysis) tests were conducted, between the temperature range of 25-degree centigrade to 690-degree centigrade. The results showed a higher thermal resistance of G.C. with a substantially reduced mass and no decomposition of phase, as was the case with portlandite,  $Ca(OH)_2$ , in HPC (high-performance concrete). Such experimental findings help G.C. application at high temperature, which is limited to 400-degree centigrade in HPC. **Jagmohan Vijay Jandhyala et al. [7]** investigated bricks made from Phosphogypsum, Fly-ash and alkaline solution, subjected to drying in a hot air oven. This study led to the following conclusions. The lowest compressive strength of these bricks was 7.5 Mpa; this paste mix has application in filler materials and infill walls. Bricks with a compressive strength of 12.5 Mpa and above seen in some cases may have structural applications. Compressive strength is not affected significantly by fly-ash content. However, the fly-ash content lowers both dry and wet densities. The water absorption is within the 20 % limit as prescribed by the I.S. code. These bricks may find application in liquid retaining structures. **Jagmohan Vijay Jandhyala et al. [8]** studied the effect of Phosphogypsum and fly-ash in making air-dried geopolymer bricks. The conclusions from those studies are as follows. Air curing produces compressive strength in the range of 12.5 Mpa, which has both load-bearing and non-load-bearing applications. The presence of fly-ash in the mixes gives slightly higher compressive capacities and lowered dry and bulk densities when compared with mixes without fly-ash. The non-addition of fly-ash in the mix causes the densities to go beyond 20  $kN/m^3$ , which is higher than the density of conventional masonry bricks.

### III. APPARATUS AND SUBSTANCES REQUIRED

#### A. Apparatus & Equipment

1. Conductive carbon adhesive tapes.
2. Specimen Mounts.
3. Specimen sample holder.
4. SEM. (Scanning Electron Microscope.)
5. XRD Equipment.

#### B. Substances required

##### a) Fly-ash:

60-65 % fly-ash conforming to Grade 2 as per IS 3812 was used. Ramagundam, Telangana, National thermal Power Corporation is the source of this fly-ash used.

**b) Phosphogypsum:**

Finely ground Phosphogypsum powder (Refer to Fig 1.) sourced from Coromandel fertilisers, Kakinada was used. The main elemental contents are 18 % sulphur, 22 % calcium and 3-4 % moisture.

**c) Coarse Aggregate:**

Aggregate conforming to I.S. 383:1970.

**d) Sand (Fine aggregate):**

River sand conforming to I.S. 383:1970.

**e) Sodium Hydroxide (NaOH):**

Sodium Hydroxide pellets of 99% concentration with a molarity of 10 were used to make the alkaline solution (Refer Fig 2.)



**Fig 1: Finely ground Phosphogypsum.**



**Fig 2: Sodium Hydroxide pellets.**

**f) Sodium silicate (Na<sub>2</sub>SiO<sub>3</sub>):**

10 Molar sodium silicate was used for making an alkaline solution. (Refer Fig 3.)



**Fig 3: Sodium silicate crystals.**

**IV. EXPERIMENTAL PROCEDURE**

**A. Procedure**

Mixes (paste) were made by combining Phosphogypsum, Fly-ash and alkali solution (sodium hydroxide and sodium silicate). Some Bricks have been without fly-ash. Samples made with fly-ash were called 'S1', and those samples made without fly-ash were called 'S2'.

The S1 and S2 samples have been subject to microstructure testing tools like SEM analysis and Powder X-ray Diffraction (PXRD). The microstructure properties obtained from SEM analysis were used to corroborate the

macrostructure properties, published in earlier papers by **Jagmohan Vijay Jandhyala. et.al. [7,8]**. (Refer Table 1.)

**a) Sample Preparation for SEM (Scanning Electron Microscope) Analysis**

1). The sample material has been subjected to evaporative drying inside a vacuum chamber to eliminate all moisture content. The presence of moisture may intervene with the SEM and PXRD signals. (Fig: 4).

2). Next, 1 cm x 1 cm samples of each material were made and placed in a circular specimen mount, along with several such specimens. (Fig: 5). The samples on the mould were covered by conductive carbon tape. Several such moulds are required.



**Fig 4: Vacuum Drying Chamber**



**Fig 5: SEM Sample Specimen mount preparation.**

3). The mould was placed inside the SEM, and the images of various specimens have been taken at different voltages (electrical conductivity) and resolutions. (Fig: 6).

4). The images obtained have been studied, analysed and inferences have been drawn.



**Fig 6: Scanning electron microscope.**

**2) Sample Preparation for X-Ray Diffraction (PXRD)**

1). The sample material has been subject to evaporative drying inside a vacuum chamber to eliminate all moisture content. The presence of moisture may intervene with the SEM and PXRD signals.

2). Next, a sample of each material to be tested is made and placed in a circular specimen holder. But unlike SEM analysis, only one specimen is tested in each cycle of PXRD (Fig: 7). Several such moulds are required.

- 3) The moulds have been placed inside the x-ray diffraction machine, and the spectra of the specimen are taken. (Fig: 8).
- 4) The procedure from steps 1-4 have been repeated for each specimen individually.
- 5) The x-ray diffraction spectrums obtained have been studied, analysed and inferences have been drawn.



Fig 8: X-ray diffraction device



Fig 7: PXR Sample Specimen mount preparation.

## V. Results and Inferences

### A. Results

TABLE 1: Brick Properties Vs Percentages of Phosphogypsum and fly-ash that have been obtained from previously published papers by Jagmohan Vijay Jandhyala. et al. [7,8] are presented in table no 1.

S.L. NO.	“PERCENTAGE OF PHOSPHOGYPSUM IN SAMPLES 1 & 2”	“COMPRESSIVE STRENGTH (S1), MPA”	“% WEIGHT GAIN (WATER ABSORPTION) (S1).”	“DRY DENSITY (S1) IN KG/M <sup>3</sup> ”	“BULK DENSITY (S1) IN KG/M <sup>3</sup> ”	“PERCENTAGE OF FLY-ASH IN SAMPLE 1”	“COMPRESSIVE STRENGTH (S2), MPA”	“% WEIGHT GAIN (WATER ABSORPTION) (S2).”	“DRY DENSITY (S2) IN KG/M <sup>3</sup> ”	“BULK DENSITY (S2) IN KG/M <sup>3</sup> ”
1	9	20.31	17.81	1670.36	1967.84	9	17.11	17.17	2010.36	2312.18
2	10	21.78	17.61	1669.79	1963.85	10	18.12	17.77	2000.22	2280.23
3	11	22.65	17.56	1669.16	1962.24	11	18.91	18.05	1998.34	2270.67
4	12	22.95	17.73	1668.46	1964.21	12	19.11	18.17	1968.88	2262.92
5	13	23.13	17.68	1667.69	1962.48	13	19.18	18.28	1908.22	2259.92
6	14	23.06	17.66	1666.82	1961.29	14	20.37	18.62	1905.59	2260.28
7	15	22.85	17.66	1665.85	1960.03	15	20.97	18.68	1902.63	2258.03
8	16	22.49	17.68	1664.75	1959.07	16	21.11	18.66	1899.27	2253.67
9	17	21.95	17.7	1663.49	1957.83	17	21.08	18.64	1895.43	2248.79
10	18	21.27	17.67	1662.03	1955.73	18	21.04	18.67	1891	2244.10
11	19	20.49	17.68	1660.33	1953.81	19	21.1	18.67	1885.83	2237.92
12	20	19.58	17.69	1658.33	1951.64	20	21.15	18.67	1879.73	2230.64
13	21	18.6	17.67	1655.92	1948.39	21	20.99	18.69	1872.4	2222.35
14	22	17.56	17.57	1652.98	1943.38	22	20.7	18.64	1863.44	2210.84
15	23	16.38	17.61	1649.3	1939.69	23	19.42	18.68	1852.25	2198.29
16	24	15.22	18.18	1644.57	1942.8	24	18.73	18.69	1837.86	2181.36
17	25	15.13	18.47	1622.17	1942.8	25	17.45	18.75	1818.67	2157.92
18	MAX	23.13	18.47	1670.36	1967.84	MAX	21.15	18.75	2010.36	2312.18
19	MIN	15.13	17.56	1622.17	1939.69	MIN	17.11	17.17	1818.67	2157.92
20	AVG	20.32	17.74	1659.53	1955.12	AVG	19.80	18.44	1905.30	2240.59

TABLE 2: Percentages of elements in various samples obtained from X-ray diffraction studies are presented in table no 2.

Element	S1(I)	S1(ii)	S1(iii)	S1(iv)	AVG(S1)	S2(a)	S2(ii)	S2(iii)	S2(iv)	AVG(S2)
OXYGEN	19.1	21.2	19.6	20.2	20	18.9	18.1	19.6	19.3	19
SODIUM	6.3	5.9	6.1	5	5.8	9.1	8.6	8.6	7.8	8.5
ALUMINIUM	2.7	2.3	1.9	2.5	2.4	1.7	1.4	2.1	2.1	1.8
SILICON	18.2	15.9	16.2	18.1	17.1	21.5	25.3	23.2	25.7	23.9
PHOSPHOROUS	5.3	5.4	4.8	5.5	5.3	8.9	8.1	8.9	8.4	8.6
SULPHUR	20.7	20.3	22	20.7	20.9	13.2	13.8	10.9	12.1	12.5
CALCIUM	25.8	22.9	24.5	22.7	24	19.1	17.3	18.4	18.3	18.3
CARBON	2	5.9	4.9	5.3	4.5	9.1	5.7	9.2	6.4	7.6

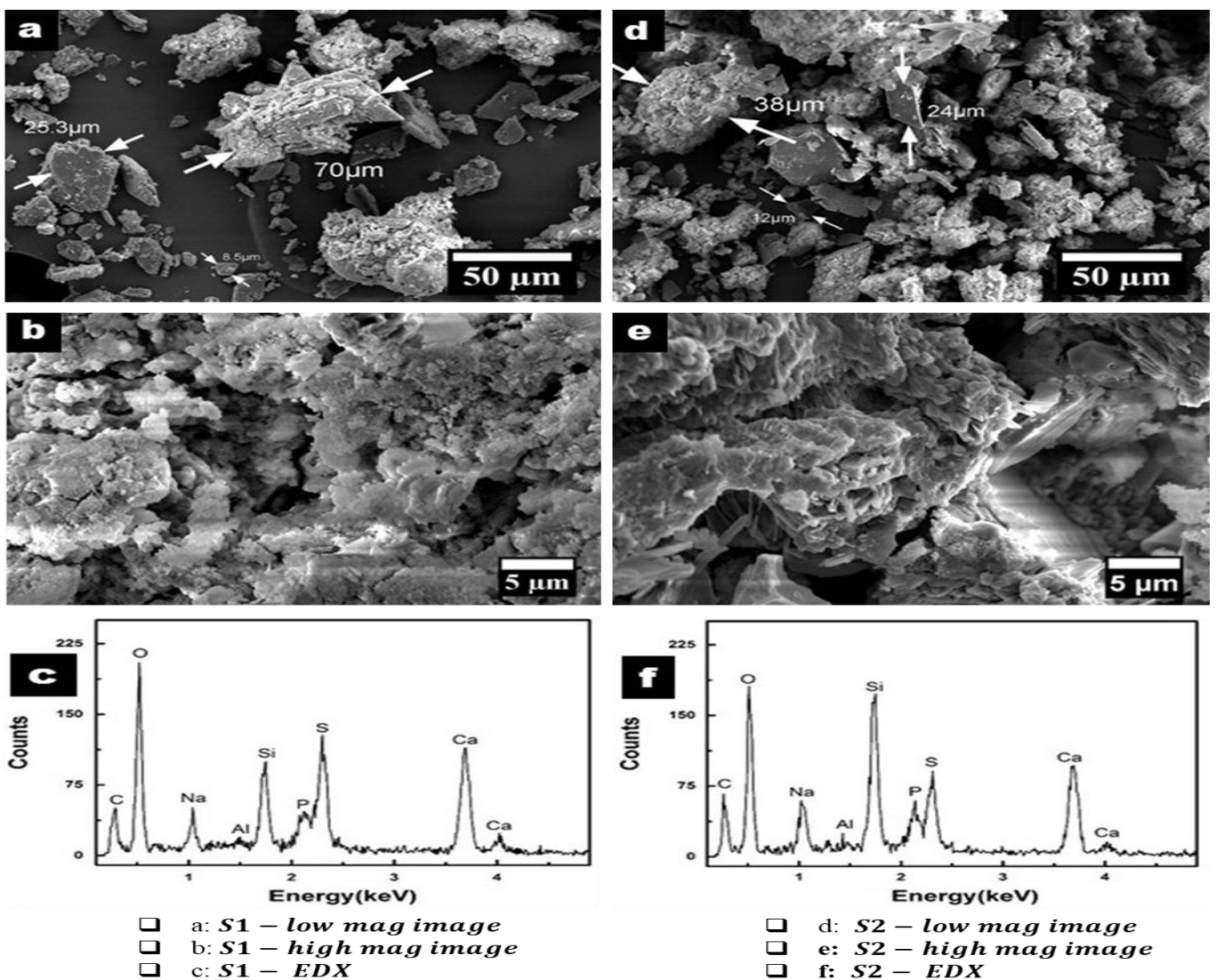


Fig 9: Showing low, high magnification images and EDX spectra of samples S1 and S2.

**B. Inferences & Interpretation**

- Figure 9(a) shows the low magnification image of the S1 specimen.
- The specimen consists of a randomly shaped microstructure with a size varying from a few

micrometres to a maximum of 70  $\mu\text{m}$ , as shown in the figure.

- To look at the surface of each such microstructure, images were taken at significantly higher magnifications. One such high magnification image has been shown in figure 9(b).
- The surface of each microstructure looks highly porous, suggesting that these microstructures are clusters of hundreds of nanoparticles. Such a structure is usually known to give high porosity for any material. (Figure 9(b).)
- Figure 9(d) shows a low magnification image of S2.
- When compared to the S1 image at the same magnification (Figure 9(a)), it was seen that the number of microstructures has increased.
- Careful observation reveals that the average size of available microstructures has decreased considerably. Size has been seen to range between 12  $\mu\text{m}$  to 38  $\mu\text{m}$  in this particular area.
- By comparing figures 9(a) and 9(d), it was inferred that the average size of microstructures has decreased in S2. In figure 9(e), the S2 specimen has also been showing porous surface morphology, which has also been seen in the case of S1 (Figure 9(b)).
- To know the chemical composition of specimen S1, EDX scans were taken at different locations. One such representative EDX spectrum has been shown in Figure 9(c).
- EDX spectrum shows that the S1 specimen contains a host of elements, including carbon, oxygen, sodium, silicon, sulphur and calcium. It has also shown trace amounts of aluminium as well. (Refer to table 2.)
- To know any morphological difference between S1 and S2, high magnification images of S2 specimen have been taken, similar to images taken in the case of S1 specimen. The corresponding EDX spectrum (Figure 9(f)) also shows the same elements as seen in the case of S1 (Figure 9(c)).
- However, careful measurement reveals that the elemental percentage changes substantially between S1 and S2.
- EDX scans for four different specimens for each of the samples, S1(Figure 10) and S2(Figure 11), have been taken to obtain statistically accurate data. Then, the elemental percentage for each specimen was tabulated, and average values were calculated as shown in table no: 2 above.
- According to this table, oxygen percentage does not change much between S1 and S2.
- Sodium content has increased from 5.8% to 8.5%.
- Silicon content has increased from 17.1% to 23.9%
- Phosphorous content has risen from 5.3 % to 8.6%
- Interestingly, other major elements such as Sulphur and Calcium have shown a substantial decrease. Sulphur decreases from 20.9% to 12.5%, whereas calcium decreases from 24% to 18.3%.

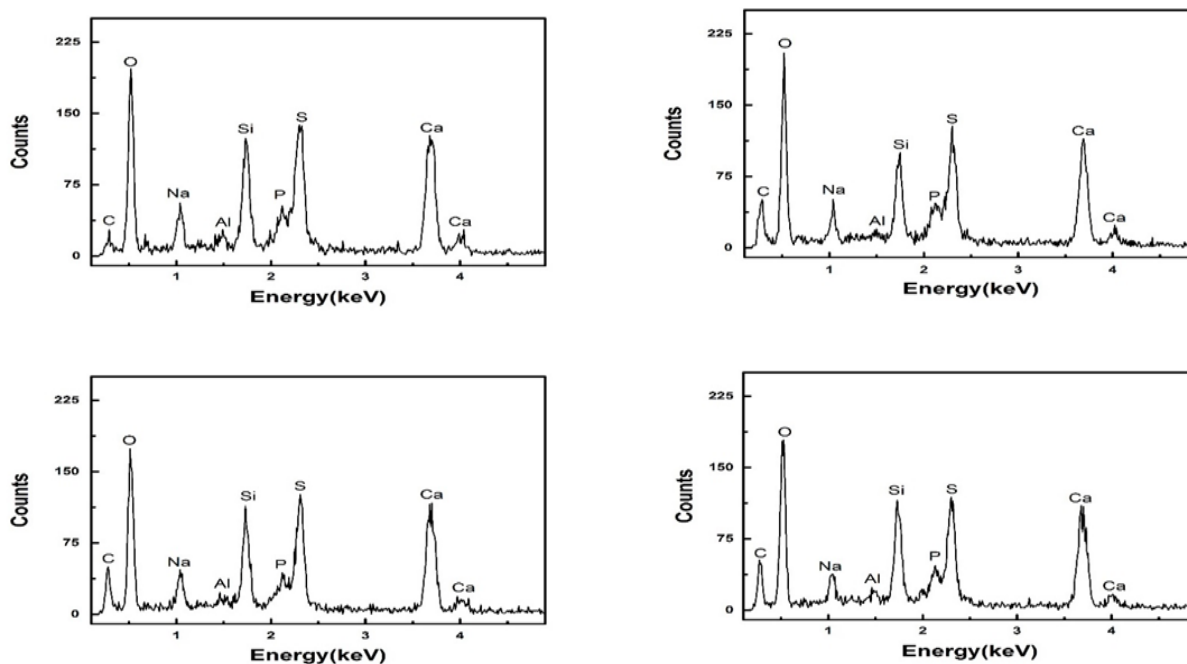


Fig 10: Showing Sample 'S1', Xray-diffraction spectrums.

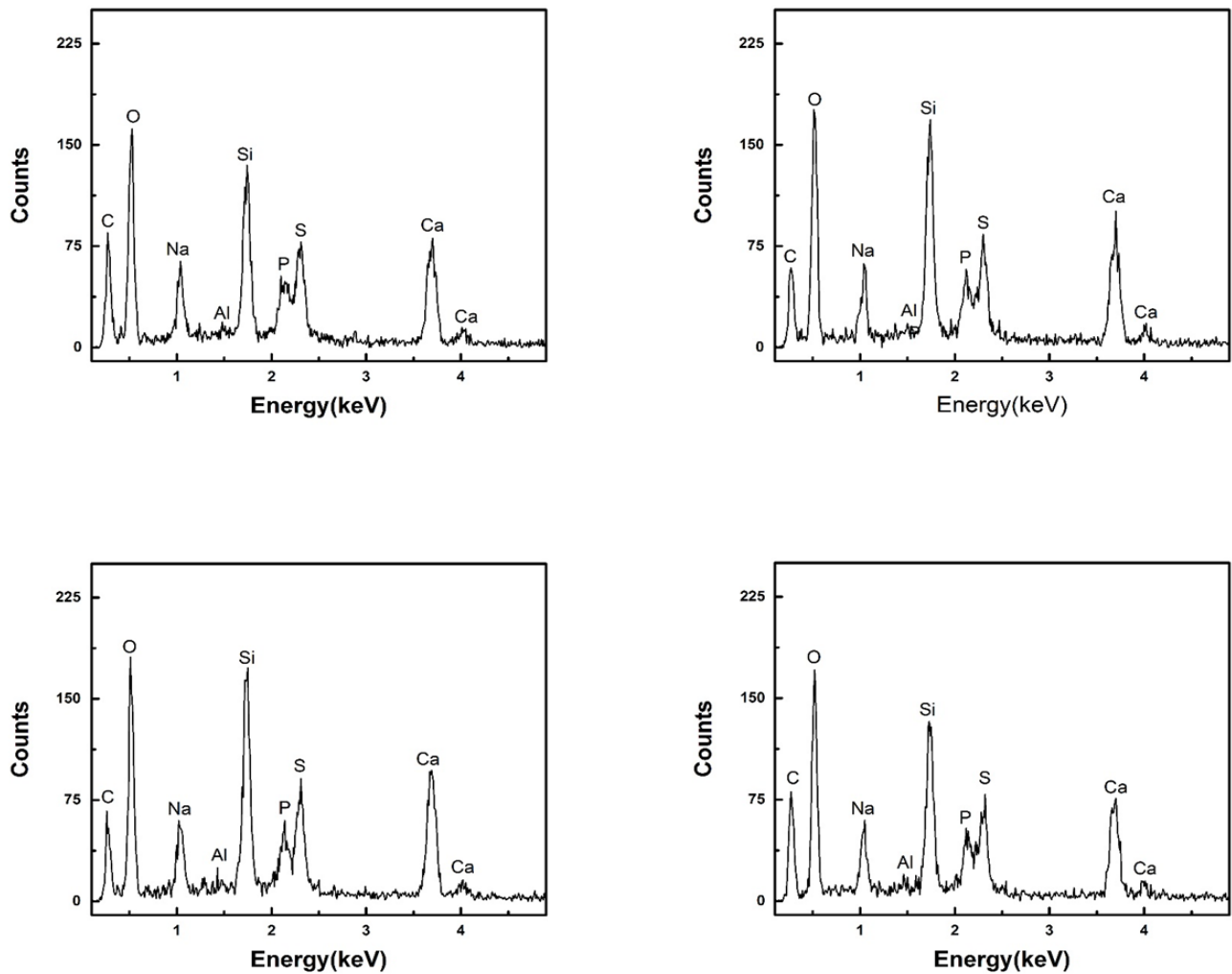


Fig 11: Showing sample S2, Xray diffraction spectrum.

C. Brick Properties correlated to SEM and EDX.

TABLE 3: Silicon to the Aluminium ratio in different sample specimens obtained from x-ray diffraction analysis are presented in table 3.

Element/Ratio	'S1'(i)	'S1'(ii)	'S1'(iii)	'S1'(iv)	AVG	Element/Ratio	'S2'(i)	'S2'(ii)	'S2'(iii)	'S2'(iv)
SILICON	18.2	15.9	16.2	18.1	17.1	21.5	25.3	23.2	25.7	23.9
ALUMINIUM	2.7	2.3	1.9	2.5	2.4	1.7	1.4	2.1	2.1	1.8
SILICON: ALUMINIUM	6.74	6.91	8.53	7.24	7.13	12.65	18.07	11.05	12.24	13.28
	MAX	8.53				MAX	18.07			
	MIN	6.74				MIN	11.05			

a) Compressive Strength:

The compressive strength is higher in the case of sample S1 than in sample S2. The compressive strength in both cases is in the range of 15.13 Mpa - 23.13 Mpa. So, the higher compressive capacity mix may be used for building construction applications as well. The lower strength mixes find application as filler material and other non-structural applications. A low liquid / solid ratio and high alkaline concentration (10 M) may have been one of the

parameters affecting compressive capacity. The ratio of Si/Al (Table 3.) also plays a role in determining the compressive strength, and a lower Si/Al ratio results in higher compressive strength. In the case of sample S1, the ratio of Si/Al is lower than that of the corresponding values of S2. From table 1, it was inferred that S1 paste is having higher compressive strength than S2. It was seen that the ratio of Si/Al has been varying slightly, and at someplace, the variation is higher. Corresponding compressive strength has also been varying accordingly;

when the Si/Al ratio has been somewhat changing, the compressive strength also changes slightly. When the Si/Al ratio changes are more significant, the variation in compressive strength is also higher.

#### **b) Water absorption:**

Water absorption has been higher in the case of both samples S1 and S2. From SEM images (from figure 9(b) and 9(e)), it was inferred that hundreds of nano-sized particles are present, which may have led to a highly porous structure. These pores have been filled with water when the paste in the shape of brick was kept immersed in water for 24 hours. So, this water that has been retained in the pores leads to high water absorption.

#### **c) Dry density and Wet density:**

Wet density is higher in both samples S1 and S2; the highly porous structure leads to volumetric bulking on water absorption due to the pores getting filled with water, leading to more mass and wet density. When dry density is measured, the paste mix is totally dried, so all the water from the pores leaves the paste mix, leading to volumetric shrinkage and lower mass. Thus, the dry density also decreases and is lower than wet density.

### **VI. Conclusions and Recommendations**

Since the specimen were dispersed on conductive carbon tape, the carbon content in the specimen may not be precisely known, as the signals may also include carbon tape signals. Other studies may have to be taken up for the accurate assessment of carbon content. The various macrostructure properties with and without fly-ash have been corroborated. Samples S1 and S2 were investigated using SEM and EDX scans. The specimen consists of a randomly shaped microstructure with sizes varying from few microns to 70 microns. The structure is highly porous, leading to low densities, both dry and wet. The water absorption is due to the pore's spaces getting filled with water molecules. The higher compressive strength is due to the relatively low liquid-solid ratio using 10M alkali solution. The effect of other alkaline solutions with different molarities may be studied in further research. The impact of different pozzolanic materials like rice husk, corn waste, bagasse etc., may be explored in future research. Other studies like TGA (thermogravimetric analysis) and DSC (differential scanning calorimeter) need to be taken up to understand the geopolymer paste's micro-properties further.

### **VII. REFERENCES**

- [1] Yootaek Kim, Kyongwoo Lee, Transmission Electron Microscopic Analysis of Geopolymer Made of Fused Slags, Proceedings of the 2015 International Conference on Sustainable Energy and Environmental Engineering, (2015) 189-192. <https://dx.doi.org/10.2991/seeec-15.2015.47>
- [2] Ahmad Muhd Izzat, Abdullah Mohd Mustafa Al Bakri, Hussin Kamarudin, Ligia Mihaela Moga, Ghazali Che Mohd Ruzaidi, Mohd Tahir Muhammad Faheem, Andrei Victor Sandu, (2013), Microstructural Analysis of Geopolymer and Ordinary Portland Cement Mortar Exposed to Sulfuric Acid. *Materiale Plastice*. September, 50. <https://www.mdpi.com/1996-1944/12/19/3115>.
- [3] Abideng Hawa, Danupon Tonnayopas, Woraphot Prachasaree, Performance Evaluation and Microstructure Characterization of Metakaolin-Based Geopolymer Containing Oil Palm Ash", Hindawi Publishing Corporation, The Scientific World Journal Volume 2013, Article ID 857586, 9 pages. <http://dx.doi.org/10.1155/2013/857586>.
- [4] Oliver Vogt, Neven Ukrainczyk, Conrad Ballschmiede and Eddie Koenders, Reactivity and Microstructure of Metakaolin Based Geopolymers: Effect of Fly Ash and Liquid/Solid, *Materials* 12(21) 3485. <https://doi.org/10.3390/ma12213485>.
- [5] Mandeep Kaur, Jaspal Singh, Manpreet Kaur, " Microstructure and strength development of fly ash-based geopolymer mortar: Role of nano-metakaolin", *Construction and Building Materials*, Volume 190, 30 November (2018) 672-679. <https://doi.org/10.1016/j.conbuildmat.2018.09.157>
- [6] Diegles Simoes de Toledo Pereira, Felipe Jose da Silva, Ana Beatriz Rodrigues Porto, Veronica Scarpini Candido, Alisson Clay Rios da Silva, Fabio Da Costa Garcia Filho, Sergio Neves Monteiro, "Comparative analysis between properties and microstructures of geopolymer concrete and Portland concrete", *Journal of Materials Research and Technology*, 7(4) (2018) 606-611, <https://doi.org/10.1016/j.jmrt.2018.08.008>
- [7] Jagmohan Vijay Jandhyala, Prof. H. Sudarsana Rao, Prof. Vaishali. G. Ghorpade, "Feasibility Study on Production of Geopolymer Masonry Bricks with Phosphogypsum and Fly Ash (Oven-Dried)", *International Journal of Engineering Research and Technology*. ISSN 0974-3154, 13(6) (2020) 1330-1343. <https://dx.doi.org/10.37624/IJETT/13.6.2020.1330-1343>
- [8] Jagmohan Vijay Jandhyala, Prof. H. Sudarsana Rao, Prof. Vaishali. G. Ghorpade, Geopolymer Masonry Bricks production using Phosphogypsum and Fly Ash (Air-Dried samples) – A Detailed Feasibility study, *International Journal of Engineering Research and Technology*. ISSN 0974-3154, 13(12) (2020) 4758-4772. [http://irphouse.com/ijert20/ijertv13n12\\_97.pdf](http://irphouse.com/ijert20/ijertv13n12_97.pdf)
- [9] Blesson Mathai, Prof. Cijo Mathew, Prof. Pratheesh K, Dr Cibu K Varghese, Effect of Silicon on Microstructure and Mechanical Properties of Al-Si Piston Alloys, *International Journal of Engineering Trends and Technology (IJETT)*, V29(6),299-303 November 2015. ISSN:2231-5381. [www.ijettjournal.org](http://www.ijettjournal.org). Published by seventh sense research group. <https://dx.doi.org/10.14445/22315381/IJETT-V29P256>
- [10] C.E Akili, M. Alami, A. Bouayad, Article: Cooling Rate Effect Study on the Microstructure and Hardness of Hypereutectic Aluminium Al-18%Si Elaborated by V-process, *International Journal of Engineering Trends and Technology (IJETT)*, 7(2),65-70, published by seventh sense research group. <https://dx.doi.org/10.14445/22315381/IJETT-V7P233>
- [11] S.A Tukur, M. M Usman, Isyaku Muhammad, N. A Sulaiman, Effect of Tempering Temperature on Mechanical Properties of Medium Carbon Steel, *International Journal of Engineering Trends and Technology (IJETT)*, V9(15) (2014) 798-800. ISSN:2231-5381 [www.ijettjournal.org](http://www.ijettjournal.org). published by seventh sense research group. <https://dx.doi.org/10.14445/22315381/IJETT-V9P350>
- [12] Anu Saini, Ashok Kumar, Vijay Kumar Anand, Suresh Chander Sood, "Synthesis of Graphene Oxide using Modified Hummer's Method and its Reduction using Hydrazine Hydrate", *International Journal of Engineering Trends and Technology (IJETT)*, V40(2) (2016) 67-71. ISSN:2231-5381. [www.ijettjournal.org](http://www.ijettjournal.org). published by seventh sense research group. <https://dx.doi.org/10.14445/22315381/IJETT-V40P211>